

## Short communication

# Coastal circulation within the Banks Peninsula region, New Zealand

JANELLE V. REYNOLDS-FLEMING

University of Canterbury/National Institute for  
Water and Atmospheric Research Limited  
Centre for Excellence in Marine Ecology  
and Aquaculture  
10 Kyle Street  
Christchurch, New Zealand  
email: [jv.fleming@niwa.co.nz](mailto:jv.fleming@niwa.co.nz)

JASON G. FLEMING

National Institute for Water and Atmospheric  
Research Limited  
10 Kyle Street  
Christchurch, New Zealand  
email: [j.fleming@niwa.co.nz](mailto:j.fleming@niwa.co.nz)

## INTRODUCTION

Banks Peninsula, a protrusion off the eastern coast of South Island, New Zealand, is an extant volcanic landmass of c. 1170 km<sup>2</sup> (Fig. 1). This peninsula is mainly composed of basaltic reefs with many bays and harbours formed by volcanic venting (Sewell 1988). It was initially an offshore island, but attached to the mainland of South Island during interglacial variations in sea level as alluvial fans of the Canterbury Plains extended the eastern front (Brown & Wilson 1988). The result is a rocky reef headland that juts out to within 40 km of the continental shelf break and is bracketed to the north and south by sand and cobblestone beach habitats.

The patchiness and abrupt changes in geomorphology and biogeography of the Banks Peninsula region make it an ideal example for studying transport of nutrients, larvae, and sediment. The Banks Peninsula/Pegasus Bay region is also intrinsically interesting owing to a variety of anthropogenic influences. Both local and international fishing vessels heavily fish the region during the spring and summer and the coastal areas are subject to sewage outfall and mussel farm operations. Therefore, basic research on coastal circulation and transport in this region can also aid environmental councils and managers in decision making for the public.

Like most neritic waters, nearshore transport around Banks Peninsula is a combination of tidal, wind-driven, freshwater and differential heating induced baroclinic currents along with influences from oceanic currents (Csanady 1981). However, the particular combination of influences that governs the nearshore flow around Banks Peninsula has not been determined; until now, no long-term nearshore instrument deployments had been completed anywhere in the region. In contrast, the dominant open ocean currents off the Canterbury continental shelf have received some attention (Heath 1985). In particular, the main oceanic current which may influence peninsular circulation is the Southland Current/Front, which is believed to have its origin in the subtropical convergence west of New Zealand

**Abstract** The transport of nutrients, larvae, and sediment around coastal headlands critically depends on the balance of forces that direct the currents very near to the shore. The Banks Peninsula region, New Zealand, was selected to study nearshore circulation around coastal headlands. The relative influences of tides and wind on the current were determined using an acoustic Doppler current profiler (ADCP) deployed 2 km offshore in Pegasus Bay. Results indicated that the M<sub>2</sub> tide is the dominant tide and explains 30% of the variance. Low frequency variability was strongly correlated with wind in the offshore direction and explained a further 20–40% of the variability. Finally, mean residual flows were 2 cm/s southward along shore, which supports the hypothesis that an eddy is episodically present in Pegasus Bay. This study is the first to quantitatively document the nearshore circulation in the Banks Peninsula region.

**Keywords** Banks Peninsula; Pegasus Bay; coastal circulation; tidal currents; wind-driven currents; ADCP

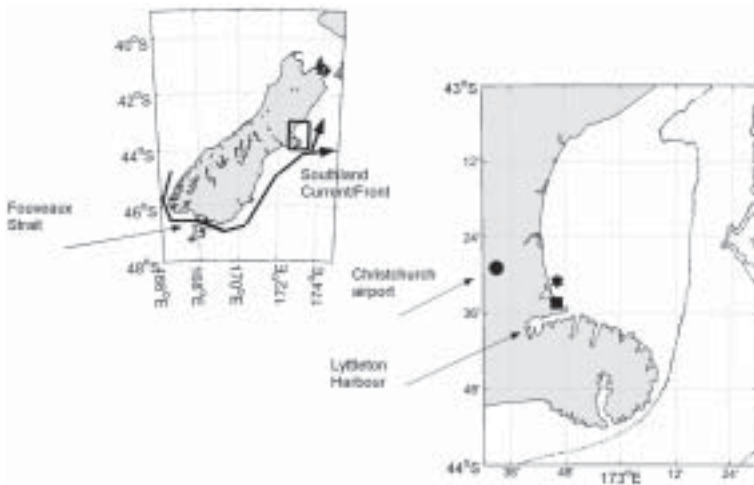


**Fig. 1** South Island, New Zealand and the Banks Peninsula study site. Southland Front/Current is represented by a thick arrow. Bathymetric contours are 50 m, 100 m, and 200 m. (\*, location of the acoustic Doppler current profiler (ADCP).)

(Heath 1972; Chiswell 1996). This persistent current flows along the continental shelf through Foveaux Strait, around the south-east tip of New Zealand and along the continental shelf break of the east side of the South Island, eventually forking into two directions just after Banks Peninsula (Fig. 1). Studies of the variability within the current have been conducted (Chiswell 1996), although its influence on nearshore circulation around Banks Peninsula has not been quantitatively established.

Some efforts in this regard include drifter studies, which have shown that drift cards released south of the peninsula tend to pool and that shore recovery of drifters was most intense along Pegasus Bay beaches on the north side of Banks Peninsula (Heath & Shakespeare 1977; Carter & Herzer 1979; Jenks et al. 1982). Carter & Herzer (1979) interpreted their drift card data in conjunction with two *Landsat* photographs and concluded qualitatively that an eddy may be present at times in Pegasus Bay, although wind forcing is probably also important there and that “apparently, the circulation within the bay is complex and variable” (Carter & Herzer 1979).

The drift card studies produced by Carter & Herzer (1979) and the offshore Southland Current measurements by Chiswell (1996) are the only transport-related physical oceanography work to-date in the Banks Peninsula region. The other previous physics studies in this region will be summarised here for completeness. A study of sea surface temperature (SST) at sites around New Zealand (including Lyttelton Harbour (see Fig. 1)) described seasonal variation as well as daily standard

deviations and comparisons with air temperature (Greig et al. 1988). A study by (McKendry et al. 1988) used Lyttelton SST and a mesoscale wind model with a 10-km grid spacing to conclude that strong north-westerly winds may be responsible for unusually deep transient depressions in SST in the region. In addition, remotely sensed SST was used to infer flow of the Southland Current through the Mernoo saddle (c. 200 km east of Banks Peninsula) and into the region north of Pegasus Bay (Shaw & Vennell 2000). Finally, sea level data from six locations along the Canterbury coast were analysed and indicated persistent waves with periods of 3.4 h in Pegasus Bay (Goring & Henry 1998). These waves were thought to be edge waves and, in Pegasus Bay, they are trapped laterally between the northern extent of the bay and Banks Peninsula and offshore by the shelf.

In summary, the results of previous coastal physics work in the Banks Peninsula region have generally been far too remote and too coarse in time and spatial resolution to provide any insight into the transport of nutrients, larvae, or sediment near the shore in the Banks Peninsula region. In Pegasus Bay in particular, the complex and time varying balance of influences from tides, winds, and long-term residual flows has not been addressed in any previous work. Although remotely sensed SST images have been used to determine the large-scale oceanic features around New Zealand (Uddstrom & Oien 1999), daily composite images of this much smaller area cannot be used to discern the high frequency circulation near the coast. This is in part because of chronic cloud cover over the study area

(Uddstrom & Oien 1999) and a mismatch between temporal sampling of remotely sensed SST (where a sample results from a 24-h composite image) and the time scale of tidal advection. Finally, it is very difficult to obtain accurate remotely sensed SST within 5 km of shore.

As a result, data from an Acoustic Doppler Current Profiler (ADCP) deployment within 2 km of the shore in Pegasus Bay was analysed to: (1) determine the quantitative contribution of tides, wind, and low frequency residual to the observed velocity profiles; and (2) determine whether or not there is quantitative evidence to support the hypothesis of an eddy in Pegasus Bay.

## METHODS

An RDInstruments 1200 kHz Broadband upward looking ADCP was deployed in Pegasus Bay at 43°31'S, 172°46'E from 29 January, 1999 until 11 April, 1999 (see Fig. 1). The ADCP was programmed to record ensemble averages every 10 min in 1-m vertical bins with an individual ping standard deviation of 3.0 cm/s (40 samples per average).

Velocity from the ADCP was broken into alongshore and offshore components based on a counterclockwise rotation of 20°. With this rotation, positive alongshore and positive offshore currents were defined as northward and offshore respectively. The data were demeaned and de-trended to satisfy the stationary requirement, and the major tidal constituents and their contribution to the variance in the flow were assessed using  $t_{\text{tide}}$  in MATLAB (Pawlowicz et al. 2002). A modified FFT algorithm was used for spectral analysis to partition the variance in the velocity data based on frequency. The upper bins (13–16 m above bottom (mab)) have been excluded from the analysis because of the discontinuous velocity record resulting from varying water levels associated with the tides.

Additional bivariate analysis was conducted to determine the coherences between de-tided velocity and wind at a range of frequencies. Hourly wind direction and speed data from the Christchurch airport were available through the NIWA climate database and were acquired for the deployment period to determine the correlation between wind and the de-tided current velocity profile. Non-rotated wind vectors were computed and graphed for visual comparison with the ADCP velocity field. For statistical comparison, however, wind velocities rotated in the alongshore/offshore direction were

used, following the same angular rotation used for the water velocity data. Note that the offshore wind velocities are closely aligned with the NE/SW direction, which is the dominant wind direction during summer (URS 2001).

A pressure sensor was located on the ADCP and collected water level approximations every 10 min at the ADCP location (Fig. 1).

## RESULTS

A 6-day subsample of the data was selected to provide a detailed illustration of the dynamic interaction of the wind and tides (Fig. 2) that was alluded to in Carter & Herzer (1979). The wind record began with a wind event (31 January – 2 February) followed by quiescent winds (3–5 February). The representative sample illustrates the typical response of the current to this sort of wind event: flow velocity is predominately oriented in the alongshore direction with speeds between –30 and 30 cm/s, however peaks in the offshore direction occur (i.e., during 31 January). In the middle of the day of 31 January, the wind switched direction from onshore to offshore winds. The flow velocity responded by switching from southward onshore flow to northward offshore flow. Flow is not uniform in the vertical, however, and vertical stratification is evident in both velocity orientations.

During the quiescent wind period, the tidal influence on the velocity is revealed. Specifically, during ebb tides, flow is strongly southward (>20 cm/s) and weakly offshore (<10 cm/s) whereas during flood tides, flow is predominately northward (10–20 cm/s) and weakly onshore (<10 cm/s). Periods of vertical stratification in the flow occur with a break in flow directions at c. 10 m above the bottom (i.e., noon 3–4 February). There is also an asymmetry in the flow velocities in response to the tide stage as southward alongshore velocities are longer in duration during the ebb tides than northward alongshore flow during flood tides. For estimating transport, this example shows flow speeds that are generally less than 30 cm/s in both directions. The exception is higher speeds that are recorded in the near surface (13–15 mab) and reflect the wind influence referred to earlier.

For the whole deployment period, the dominant tidal constituents and their contribution to the observed velocity profile were calculated. According to the contours of power spectral density (Fig. 3) for the alongshore and offshore velocity components,

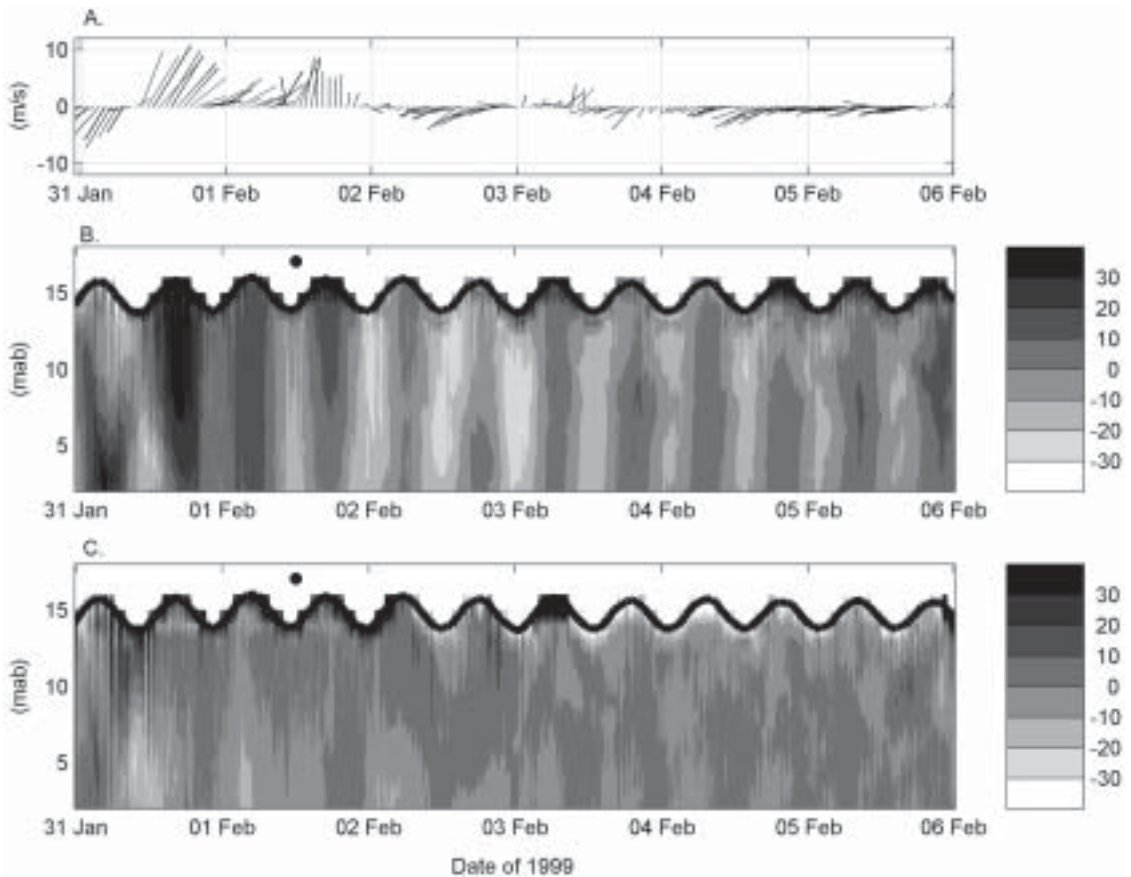


**Fig. 2** A, Wind vectors from the Christchurch airport. Contours (cm/s) of B, offshore component of velocity, and C, alongshore component of velocity for a 5-day period beginning 31 January 1999. Thick black line at the surface represents water depth from the acoustic Doppler current profiler (ADCP). (●, time of a full moon.)

the dominant semidiurnal tides are the  $M_2$ ,  $N_2$ , and  $S_2$  and the dominant diurnal tides are  $O_1$  and  $K_1$ . These tidal constituents were also shown to be the most important constituents in a study of velocity data from deeper ocean sites all around New Zealand (Stanton et al. 2001). A clear peak in the power spectra (the 3.5 contour of  $\log_{10}[\text{cm/s/cph}]^2$ ) is evident at all depths in the semidiurnal frequency range, which incorporates the  $M_2$ ,  $N_2$ , and  $S_2$  tidal components. Heightened energy is evident in the diurnal frequency range, but it is less pronounced than for the semidiurnal frequency range.

The percentage of variance in the flow as a result of the significant tidal constituents at each vertical depth is summarised in Table 1. Tidal influence is strongest in the alongshore component of velocity and a depth average of 30% of the flow variance in this component is explained by the tides. Flow

variance in the offshore component of velocity because of the tides is much weaker and averages 6% across depth. The vertical profile of tidal contribution indicates a weak relative influence at the surface that increases to a maximum at the bottom; this pattern holds for both components. For example, the tidal contribution to velocity in the offshore direction ranges from a low of 2.4% at 11 mab to a maximum of 16.8% at 2 mab. The tidal contribution to velocity in the alongshore direction ranges from a low of 16.3% at 13 mab to a maximum of 36.8% at 2 mab.

Over 90% of the flow variance of the tides is concentrated around the  $M_2$  tidal constituent. Table 1 lists the variance for the alongshore and offshore velocity components in each vertical depth bin attributed solely to the  $M_2$  tide. In the majority of examples, over 90% of the tidal variance is attributed

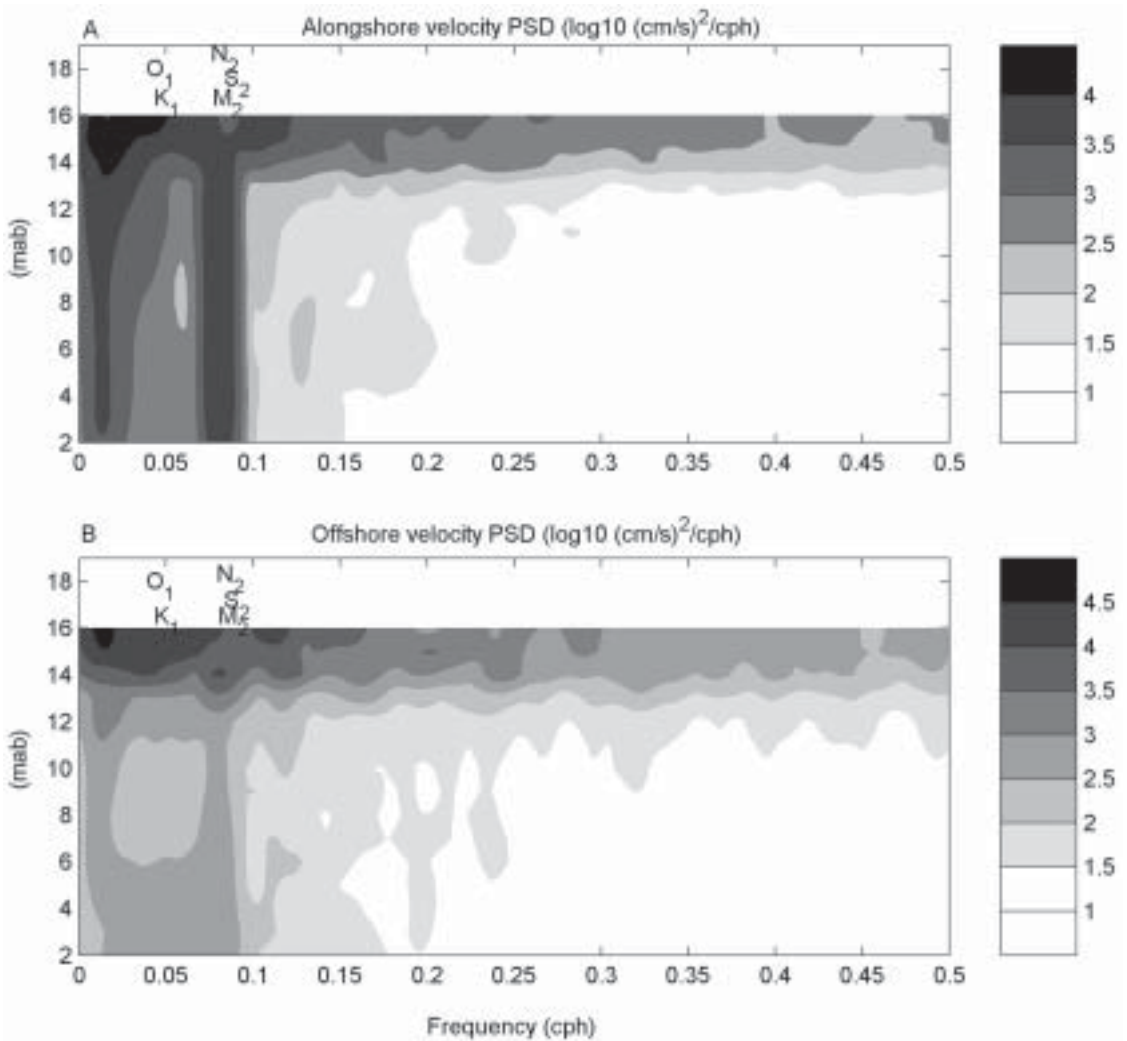


**Fig. 3** Contours  $((\text{cm/s})^2/\text{cph})$  of the power spectral density for **A**, alongshore and **B**, offshore components of velocity.

only to this semidiurnal lunar tide. The amplitude and phase information for the  $M_2$  tidal constituent for each vertical bin was calculated and the vertically varying tidal ellipses are presented (Fig. 4). The ellipses rotate in a clockwise manner with a semi-major axis of 10 cm/s, which is oriented in the alongshore direction between 2 and 11 mab. The surface ellipse has a semi-major axis oriented in the offshore direction resulting from wind forcing at the tidal frequency.

Although 30% of the variance in the flow field is attributed to tides (specifically the  $M_2$  tidal constituent), significant energy also exists in the

power spectra in both the alongshore and offshore component at lower frequencies (0–0.04 cph, Fig. 3), which is not attributable to the tides. Variance at this low frequency range often coincides with variance in atmospheric pressure systems and their associated wind fields (Csanady 1981). Coherence between de-tided velocity components and wind speeds in the alongshore and offshore direction were therefore computed to determine the possibility of a bi-variate linear relationship (Fig. 5). Strong coherence ( $>0.3$ ) between offshore wind and both de-tided velocity components is evident for the low frequency period of interest (0.01–0.03 cph; Fig. 5A,B).

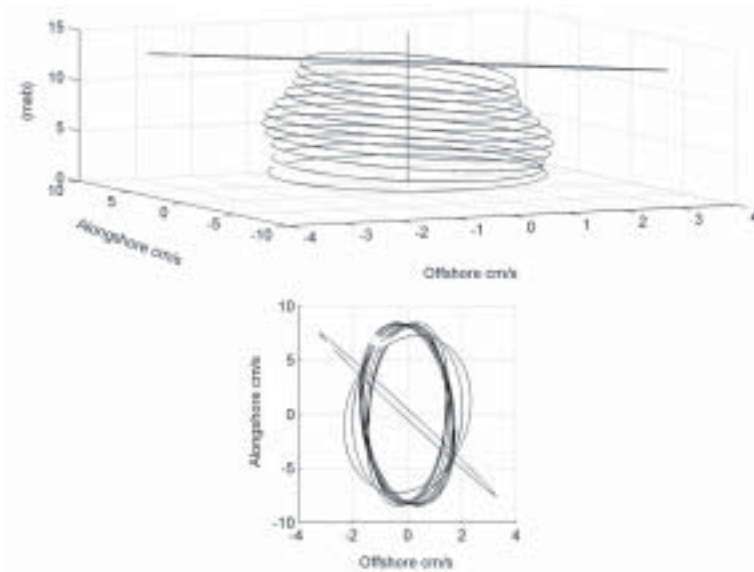


**Fig. 4** Vertical and planar views of the  $M_2$  tidal ellipses drawn from the Acoustic Doppler current profiler (ADCP) data.

**Table 1** Mean flow speeds (cm/s) for the entire 2.5 month period and percentage of the variance in flow explained by the major tidal species ( $M_2$ ,  $N_2$ ,  $S_2$ ,  $O_1$ , and  $K_1$ ) for the alongshore and offshore velocity components as well as percentage of variance in flow explained by only the  $M_2$  tidal species. (mab, m above bottom.)

Depth bin (mab)	Mean residual offshore velocity	Mean residual alongshore velocity	Major constituents offshore velocity (%)	Major constituents alongshore velocity (%)	$M_2$ only offshore velocity	$M_2$ only alongshore velocity
13.0	-1.85	2.39	6.0	16.3	5.0	16.1
12.0	-2.07	0.25	2.8	22.8	1.8	22.2
11.0	0.23	-0.85	2.4	24.6	2.4	24.0
10.0	0.23	-1.42	3.3	26.5	3.3	25.8
9.0	0.12	-1.86	4.9	28.8	4.5	27.9
8.0	0.01	-2.22	6.3	30.6	5.7	30.6
7.0	-0.11	-2.49	6.6	32.2	6.6	32.2
6.0	-0.18	-2.66	6.8	33.7	6.8	32.7
5.0	-0.09	-2.77	7.1	35.2	6.3	34.0
4.0	0.001	-2.64	10.5	35.9	6.8	34.8
3.0	0.03	-2.39	11.9	36.1	9.4	35.1
2.0	-0.07	-2.12	16.4	36.8	13.2	35.7

As expected, comparison between recorded flows and wind vectors shows that near surface waters generally flow towards the windward direction. However, coherence between offshore wind and alongshore velocity is strong ( $>0.3$ ) at low frequencies (0.01 cph) at depths between 5 and 12 mab. This is a result of water flow angled to the left of the wind direction being deeper within the water column, according to Ekman layer dynamics (Ekman 1905). Alongshore wind is also significantly coherent ( $>0.2$ ) with alongshore velocity at low

frequencies (0.01–0.03 cph) but not with offshore velocity (Fig. 5C,D). Unlike tides, wind-driven events are stochastic and the lack of significant coherence between alongshore wind and offshore water velocity may be the result of the weakness, infrequency, or short duration of alongshore wind in Pegasus Bay.

Depth averaged mean residual velocities (Table 1) indicate a southward alongshore and slightly offshore flow over the 2.5 month period. The vertical profile of the offshore component of the

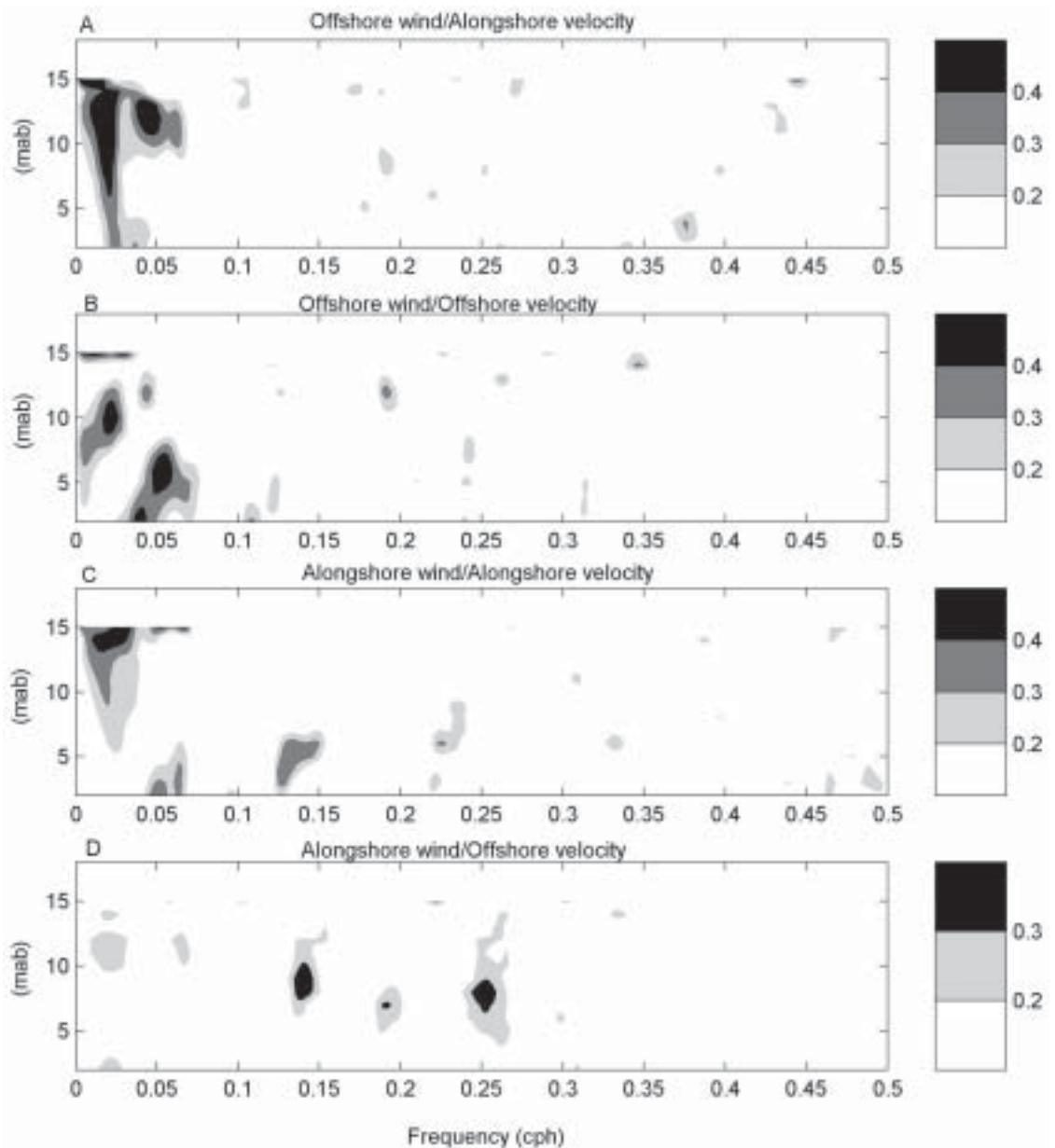


**Fig. 5** Contours of significant coherence between **A**, offshore wind and alongshore velocity; **B**, offshore wind and offshore velocity; **C**, alongshore wind and alongshore velocity; **D**, alongshore wind and offshore velocity.

residual velocity indicates landward (westerly) flow of c. 1.85 cm/s in the surface layer. Below the surface, the offshore component of residual velocities is one to three orders of magnitude smaller and variable in direction. The alongshore component of the residual velocity at the surface is northerly at 2.38 cm/s and southerly throughout the

remainder of the water column at speeds of c. 2 cm/s. The drift card study produced by Carter & Herzer (1979) reported minimum velocities of two surface drifters released in the south central region of Pegasus Bay (specifically 43°26.9'S and 173°02.1'E) of 1.5 cm/s moving west and 3.2 cm/s moving north-east.

For estimating transport from the entire deployment period, flow speeds were less than 50 cm/s over 95% of the record. Flows higher than 50 cm/s were recorded between 3% and 5% of the record and were confined to the uppermost bins, which corresponded to the near surface waters (13–15 mab).

Finally, the variance of the water level attributable to tides was also calculated. The application of  $t_{\text{tide}}$  to the sea level anomaly (SLA) or demeaned water level at the ADCP site indicated that the semidiurnal and diurnal tidal constituents were most important. These constituents represent 97.1% of the variance in the SLA.

## CONCLUSION

The patterns of physical circulation in the Banks Peninsula region have conventionally been the subject of conjecture because of the dearth of published data and analysis. This study is the first to quantitatively document this circulation and interpret the results in terms of coastal transport.

A short-term sample of the data was selected to illustrate that strong alongshore winds may dominate the flow throughout most of the water column while the wind is up. The same sample also showed that tidal forcing is reasserted throughout the water column when the wind relaxes.

An analysis of the data record as a whole highlighted the dominance of wind-driven transport at the surface and a progressive increase of tidal influence with depth. In the alongshore direction, the tides contribute 16.8% of the variance at the surface and 36.8% at the bottom. Tidal influence in the offshore velocity is weaker, contributing 6.0% of the variance at the surface and 16.4% at the bottom. The  $M_2$  tidal constituent was shown to be responsible for over 90% of the flow variance attributed to tides.

The vertical variation of the residual velocity indicates that—in the long term—surface transport of buoyant propagules, larvae, outfall plumes, and fine sediment will be northward along shore at 2.38 cm/s and landward at 1.85 cm/s. This is dramatically different to the long-term southerly alongshore transport of benthic larvae and coarse sediment at a speed of 2.12 cm/s from the same location. For larvae with long pelagic life stages and vertical migration capability, a persistent choice of depth above or below 12 mab would dramatically alter the route and resulting final habitat.

Finally, the net southerly alongshore transport indicated by the depth averaged residual velocity of

2 cm/s provides quantitative support to the hypothesis of an eddy in Pegasus Bay.

## ACKNOWLEDGMENTS

We thank Derek Goring, Roy Walters, David Schiel, and two anonymous reviewers for manuscript review and suggestions and Deborah Cox for information on the ADCP deployment as well as for the data. We also thank David Schiel and the Andrew Mellon Foundation for partial funding of the data analysis.

## REFERENCES

- Brown, L. J.; Wilson, D. D. 1988: Stratigraphy of the late Quaternary deposits of the northern Canterbury Plains, New Zealand (with an appendix by N.T. Moar and D. Mildenhall: Pollen assemblages from late Quaternary deposits in Canterbury). *New Zealand Journal of Geology and Geophysics* 31: 305–335.
- Carter, L.; Herzer, R. H. 1979: The hydraulic regime and its potential to transport sediment on the Canterbury continental shelf. *New Zealand Oceanographic Memoir* 83: 33.
- Chiswell, S. M. 1996: Variability in the Southland Current, New Zealand. *New Zealand Journal of Marine and Freshwater Research* 30: 1–17.
- Csanady, G. T. 1981: Circulation in the coastal ocean. In: Saltzman, B. ed. *Advances in Geophysics* 23. Academic Press Inc. Pp. 101–183.
- Ekman, V. W. 1905: On the influence of the earth's rotation on ocean currents. *Arkiv fur Matematik, Astronomi och Fysik* 2: 1–52.
- Goring, D. G.; Henry, R. F. 1998: Short period (1–4 h) sea level fluctuations on the Canterbury coast, New Zealand. *New Zealand Journal of Marine and Freshwater Research* 32: 119–1345.
- Greig, M. J.; Ridgway, N. M.; Shakespeare, B. S. 1988: Sea surface temperature variations at coastal sites around New Zealand. *New Zealand Journal of Marine and Freshwater Research* 22: 391–400.
- Heath, R. A. 1972: The Southland Current. *New Zealand Journal of Marine and Freshwater Research* 6: 497–533.
- Heath, R. A. 1985: A review of the physical oceanography of the seas around New Zealand—1982. *New Zealand Journal of Marine and Freshwater Research* 19: 79–124.
- Heath, R. A.; Shakespeare, B. S. 1977: Recoveries of drift cards released from oil rigs around New Zealand, 1975–76 (Note). *New Zealand Journal of Marine and Freshwater Research* 11: 393–400.



- Jenks, W. N.; Grindrod, J.; Peterson, J. A. 1982: Drift currents in the southern New Zealand region as derived from Lagrangian measurements and the remote sensing of sea-surface temperature distributions. *New Zealand Journal of Marine and Freshwater Research* 16: 359–371.
- McKendry, I. G.; Sturman, A. P.; Owens, I. F. 1988: Interactions between local winds and coastal sea surface temperatures near the Canterbury coast. *New Zealand Journal of Marine and Freshwater Research* 22: 91–100.
- Pawlowicz, R.; Beardsley, B.; Lentz, S. 2002: Classical tidal harmonic analysis including error estimates in MATLAB using T\_TIDE. *Computers and Geosciences* 28: 929–937.
- Sewell, R. J. 1988: Late Miocene volcanic stratigraphy of central Banks Peninsula, Canterbury, New Zealand. *New Zealand Journal of Geology and Geophysics* 30: 41–64.
- Shaw, A. G. P.; Vennell, R. 2000: Variability of water masses through the Mernoo Saddle, South Island, New Zealand. *New Zealand Journal of Marine and Freshwater Research* 34: 103–116.
- Stanton, B. R.; Goring, D. G.; Bell, R. G. 2001: Observed and modelled tidal currents in the New Zealand region. *New Zealand Journal of Marine and Freshwater Research* 35: 397–415.
- Uddstrom, M. J.; Oien, N. A. 1999: On the use of high-resolution satellite data to describe the spatial and temporal variability of sea surface temperatures in the New Zealand region. *Journal of Geophysical Research. C. Oceans* 104: 20729–20751.
- URS New Zealand Limited 2001: Assessment of environmental effects for Christchurch wastewater discharge. Christchurch City Council. 53 p.